A Thesis Presented to
The Faculty of Alfred University

THE SYNTHESIS, CHARACTERIZATION, AND BIOCOMPATIBILITY TESTING OF TiO_2-SUBSTITUTED SiO_2-Na_2O-CaO-P_2O_5 BIOACTIVE GLASS SCAFFOLDS

by

Lindsay Piraino

In Partial Fulfillment of
the Requirements for
The Alfred University Honors Program

May 2017

Under the Supervision of:
Chair: Dr. Anthony W. Wren
Committee Members:
Sahar Mokhtari
Dr. Matthew M. Hall

ACKNOWLEDGEMENTS

Thank you to my thesis advisor, Dr. Anthony Wren, for his guidance and input on the structure of this project, as well as his support and teaching throughout my undergraduate experience at Alfred University. Thank you to Sahar Mokhtari and Kiel Skelly for their assistance with explaining standard laboratory skills and techniques. I would also like to acknowledge my academic advisor, Dr. Matthew Hall, for his advice and recommendations for coursework scheduling and planning.

TABLE OF CONTENTS

LIST OF TABLES

Page

LIST OF FIGURES

Page

ABSTRACT

The structural properties and bioactivity were investigated for scaffolds fabricated from a series of $42SiO_2$-$24Na_2O$-$21CaO$-$14P_2O_5$ wt% glass compositions with incremental substitutions of TiO_2 for SiO_2. X-ray diffraction revealed crystallinity in the control (*Con*) and 12 wt% TiO_2 (*BG-2*) scaffolds, while the 24 wt% (*BG-4*) scaffolds had a partial amorphous nature. SEM and stereo microscopy showed an interconnected network of open pores for all three compositions with pore diameters of 516 µm, 524 µm, and 533 µm measured with optical microscopy for *Con*, *BG-2* and *BG-4*, respectively. SBF testing indicated the presence of CaP crystals on *Con* scaffolds in 15 days, but no visible deposition occurred for *BG-2* or *BG-4*even after incubation for 60 days. Analysis of ion release profiles with ICP showed a slower release rate of Si and Ca for *BG-4*, as compared to the rapid decrease followed by leveling off for *Con* and *BG-2*. Future work could investigate the mechanical properties and cytocompatibility of the scaffolds.

I. INTRODUCTION

The definition of a biomaterial has evolved over time as advances in technology and new ideas have allowed for the development of novel inventions. A biomaterial was originally defined at the Consensus Conference on Definitions in Biomaterials Science of the European Society for Biomaterials in 1987 as:

> "*a nonviable material used in a medical device, intended to interact with biological systems*[1]."

This definition was modified in 1999 to remove the nonviable restriction and confine a biomaterial's function to within the health care field. In 2010, D. F. Williams proposed a modern definition of a biomaterial as:

> "*a substance that has been engineered to take a form which, alone or as part of a complex system, is used to direct, by control of interactions with components of living systems, the course of any therapeutic or diagnostic procedure, in human or veterinary medicine*[1]."

Given the amount of time and money being invested in expanding research on improving medical technology, it would not be surprising to see further transformation of this definition in the near future[2].

Current biomaterials include several classes of materials, such as polymers, metals, ceramics, natural materials, and composites that can be used in cardiovascular, dental, orthopedic, ophthalmologic, and drug delivery practices, among other applications[3]. For example, stainless steel, titanium, and cobalt-chrome alloys have been used in joint replacements and for plates and screws for bone fracture fixation. Polyester has been used for resorbable sutures, drug delivery devices, and wound coverings while polyethylene has applications in hip and knee implants and synthetic vascular grafts. Natural materials such as collagen have been used for wound dressings and cell scaffolds[4].

This study focuses on bioactive glass, a type of biomaterial that has important applications in tissue engineering. Many tissue engineering therapies focus on the fabrication of scaffolds for regeneration of lost or damaged tissue[5]. The purpose of this research is to characterize scaffolds made of titanium-substituted bioactive glass compositions and determine the nature of ion release and calcium phosphate (CaP)

deposition in simulated body fluid (SBF).

A. Bioactive Glass

Bioactive glass is an attractive solution for solving bone fracture issues due to its ability to bond to bone, stimulation of new bone growth through ionic dissolution of the glass, biodegradability as it is replaced with natural bone tissue, and formation of a hydroxyapatite (HA) layer[6]. The standard composition of bioactive glass, 45S5Bioglass®, consisting of $45SiO_2$-$24.5Na_2O$-$24.5CaO$-$6P_2O_5$ by weight percent (wt%), was discovered by Larry Hench in 1969 at the University of Florida[7].Since then, a number of other types of bioactive glasses have been studied, including silicates based on the original 45S5 Bioglass® composition, as well as phosphate- and borate-based glasses[6].

1. Ionic Dissolution Process

When placed in biological fluid, bioactive glasses release ions into the surrounding medium. These ions have important for determining the *in vitro* and *in vivo* behavior of the biomaterial. Ionic dissolution products have been shown to stimulate the expression of genes regulating the activity of osteoblasts, leading to osteogenesis through control of the osteoblast cell cycle and proliferation[8]. Calcium and phosphorous are key ions in stimulating bone formation through increasing expression of insulin-like growth factors and matrix Gla protein, respectively[8].

Beneficial effects on antibacterial and inflammatory activity and angiogenesis have also been observed following dissolution of bioactive glasses. The outcome of incorporating different therapeutic metallic ions into the glass composition is a current area of experimental investigation[8]. Silicon is essential for metabolic processes and has been shown to increase bone mineral density and induce HA precipitation. Magnesium and strontium have beneficial effects on bone formation and strontium shows promise for treating osteoporosis. Copper is involved with angiogenesis and proliferation of human endothelial cells[9]. Figure 1 shows a summary of the biological activity of different elements that have been investigated for effects on bone formation and angiogenesis[9].

Ion	Biological activity
Si	• Metabolic processes, formation of bone tissue
	• Intake of Si increase bone mineral density
	• HAP precipitation
	• Help to stimulate collagen I formation and osteoblastic differentiation
Ca	• Favours osteoblast proliferation, differentiation and mineralisation
	• Activates Ca-sensing receptors in osteoblast cells
P	• Matrix gla protein (MGP) stimulation
Zn	• Shows anti-inflammatory effect
	• Bone formation *in vitro* by activation of protein synthesis in osteoblasts
	• Increase ATP's activity
Mg	• Help to form new bone
	• Increase bone-cell adhesion and stability
Sr	• Beneficial effects on bone formation *in vivo*
	• For treating osteoporosis
Cu	• Promote synergic stimulating effects on angiogenesis when associated with angiogenic growth factor FGF-2
	• Stimulates proliferation of human endothelial cells
B	• Stimulates RNA synthesis in fibroblast cells
	• Stimulates bone formation
Li	• treatment of both bipolar and unipolar depressive disorder
	• effects on blood and brain
	• enhance immunological activities of monocytes and lymphocytes

Figure 1: Biological activity of ions commonly found in bioactive glasses

With respect to this study, titanium was an important component of the glass composition used to create scaffolds. TiO_2 has been shown to act as a network modifier

when substituted for SiO_2, which increases the amount of non-bridging oxygen and results in greater interconnectivity when heat treated. Incorporation of higher levels of TiO_2 was also shown to increase the hardness, which would enhance key mechanical properties for load bearing applications. Crystallization was also inhibited, leading to better bioactivity and allowing for a greater number of viable mesenchymal stem cells on higher Ti-containing scaffolds[10].

Control of the ion release kinetics is necessary to ensure that specific concentrations of certain ions will be delivered in a predetermined manner. For example, while low to medium levels of calcium promote osteoblast growth and development, higher concentrations can be cytotoxic. Additionally, calcium levels in the body affect other processes besides bone metabolism, so systemic effects must be taken into consideration[8].

The ion release kinetics are determined by a number of factors related to properties of the bulk material, such as density, porosity, crystallinity, and chemical composition. Surface properties, such as the surface area, roughness, topography, and hardness, also contribute to the rate of ion release[8]. The porous nature of scaffolds increases their surface area, which may be an important variable in analyzing their ion release profile. In this study, the ion release concentrations were analyzed using Inductively Coupled Plasma-Optical Emission Spectroscopy (ICP-OES).

2. Hydroxycarbonate Apatite (HCA) Formation and Bone Bonding

While ionic dissolution products contribute to osteogenesis and bone metabolism, the formation of a hydroxycarbonate apatite (HCA) layer on the glass surface is also a mechanism of bioactivity. The process of HCA formation has five steps that occur *in vivo* or in simulated body fluid *in vitro* as follows:

i) Ion exchange of Na^+ and/or Ca^{2+} with H^+ from the solution to create silanol (Si-OH) bonds on the glass surface. Phosphate is also lost from the glass composition, leading to a silica-rich region near the surface. This is also accompanied by an increase in pH.

ii) The high pH allows for OH^- to break the Si-O-Si bonds to increase Si-OH

accumulation and increase dissolution of soluble silica.

iii) Si-OH condenses at the glass surface, causing repolymerization of the Si-O-Si network.

iv) Calcium and phosphate ions move to the surface and form a film on top of the repolymerized silica layer.

v) Hydroxyl and carbonate groups from the solution are incorporated into the CaO-P_2O_5 film, leading to a crystallized HCA layer[6].

Once the HCA layer has formed, it bonds to bone through growth factor adsorption, reducing the time needed for macrophage activity and attachment of rapidly proliferating osteoblast cells. Growth factors are able to stimulate the production of matrix proteins, which is closely followed by mineralization of the matrix, leading to osteocyte maturation and the growth of new bone[11]. Figure 2 shows an overview of the general stages on a log time scale, indicating that the initial HCA formation occurs quickly, but cellular processes take longer to develop[12].

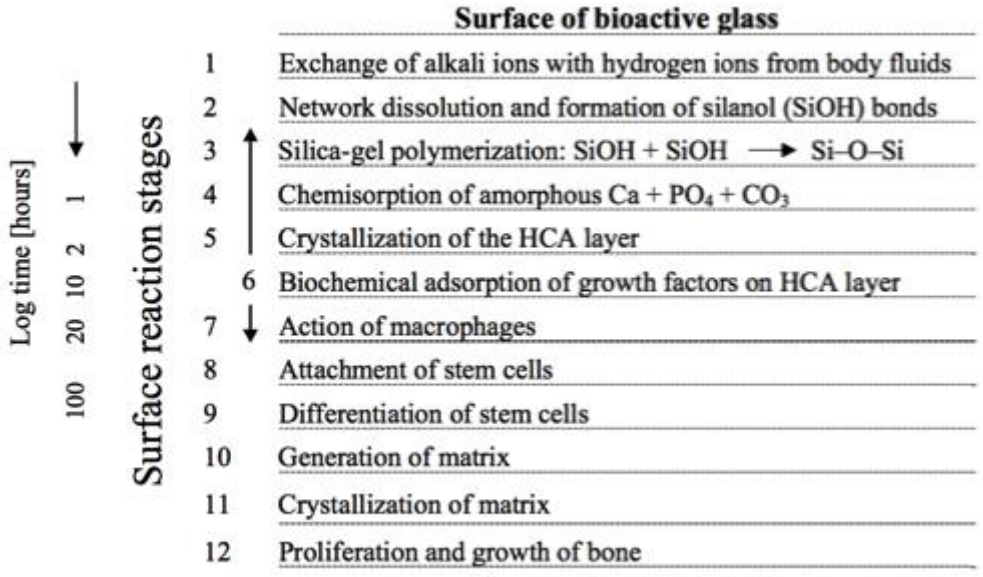

Figure 2: Stages of surface reaction on bioactive glass resulting in HCA formation

B. Bone Tissue Engineering

1. Clinical Need

Bone diseases affect around 10 million individuals in the United States and cause nearly 1.5 million fractures each year with 800,000 emergency room visits and around $18 billion spent on medical care, justifying the need to develop biomaterials to aid in bone repair. Some of the key causes of bone fracture are physical trauma, mineral deficiencies, and of bone diseases, such as osteoporosis, bone cancer, rickets, and Paget's disease[13].

Osteoporosis is of particular concern because it is the most common cause of fracture. It is prevalent in people over age 50, impacting roughly 10 million people, and the percentage of individuals over this age is increasing, thus presenting the potential to be a more significant problem in the near future. This condition is defined by low bone mass and deterioration of the bone structure, which leads to fragility and an increased risk for fracture. Diets low in calcium and Vitamin D and a lack of physical activity among older people are common contributors to the development of this disease[13].

Postmenopausal women are at the highest risk for osteoporosis, with approximately 35% of women at this age affected by the disease. Lower levels of estrogen cause the prevalence of this condition because estrogen is a key regulator of the calcium balance in bones. When calcium levels in other parts of the body fall, osteoclasts induce bone resorption to release calcium, leading to diminished bone strength[13].

2. Materials Used

Due to the high rate of bone fracture, biomaterials for bone repair are a significant advantage for the advancement of healthcare. While autologous transplantation is the best option with respect to immune response and integration, there are several key disadvantages that make it necessary to develop synthetic materials, including donor site morbidity, a limited supply of tissue, and additional pain for the patient from a second surgery to harvest the bone. Currently used biomaterials for regenerative medicine applications are inorganic materials (tricalcium phosphate, hydroxyapatite, bioactive glass), polymers (collagen, polylactic acid, polyethylene hydrogels), and biomimetic

composite materials. The use of these materials in conjunction with cells, growth factors, and/or drugs offers the potential for synergistic effects[14]. These materials can be shaped into a variety of forms to fit the particular application.

C. Bioactive Glass Scaffolds

While glass has been used in a variety of forms, including microspheres, fibers, powders, cements, and scaffolds, the porosity of scaffolds makes them the preferred structure for certain applications, allowing for the ingrowth of cells by providing increased surface area as an attachment substrate[7]. Scaffolds for bone tissue regeneration must have several key properties for optimal performance: biocompatibility, bioactivity, bone-forming ability, interconnected porosity, biodegradability, mechanical resiliency, and have the capability of being shaped for unique applications, mass produced, and sterilized[6].Cost effectiveness and production efficiency are also important considerations for using scaffolds in commercial settings[12].

Melt-derived, sol-gel-derived, and 3D printing processes can be used to make bioactive glass scaffolds; a melt-derived glass was used in this study. While many bioactive glass scaffolds are bio-ceramics, indicating that their structures are completely crystalline, it is advantageous to keep the scaffold more amorphous to preserve enhanced bioactivity of particles sintered at lower temperatures[6].

With respect to structural characteristics, an ideal bone tissue scaffold should have porosity greater than 90% to allow for permeability and ingrowth of new tissue. Pore diameters should range between 10-500 μm for proper cell seeding and nutrient and waste exchange. Micropores (<50 μm) can lead to immediate protein and cell adhesion, but higher pore sizes (>300 μm) are preferred for direct osteogenesis without the formation of an osteochondral template. However, this high degree of porosity and the degradation rate of the scaffold must be balanced with the need for mechanical durability[12].

This study tested scaffolds synthesized from a series of TiO_2/SiO_2-Na_2O-CaO-P_2O_5 glasses and evaluated their potential for successful implantation into the body. The scaffolds were characterized through x-ray diffraction, pore size measurements, and

microscopic methods. Determination of these features was followed by incubation in simulated body fluid (SBF) to assess the viability of the scaffolds in an aqueous environment through ion release and pH measurements.

II. EXPERIMENTAL PROCEDURE

A. Scaffold Synthesis

1. Glass Powder Composition

Three compositions of glass were obtained for this study, consisting of $42SiO_2$-$24Na_2O$-$21CaO$-$14P_2O_5$ wt% for the control glass (*Con*) with 12 wt% (*BG2*) and 24 wt % (*BG4*) substitutions of TiO_2 for SiO_2 in the two experimental glasses.

2. Scaffold Fabrication

Scaffolds of the three glass compositions (*Con, BG-2, BG-4*) were produced by first creating a glass slurry using the procedure reported by Wren et al. in 2012[10].Polyvinyl alcohol (PVA, 0.0007 g) was dissolved in deionized water (0.78 mL) while heating and stirring. Glass powder (1 g) was added to each flask and stirred to distribute the powder evenly. Small pieces of open cell polyurethane foam (approximately 5 mm x 5 mm x 5 mm) were cut and immersed in the slurry to coat with a thin layer of glass. The cubes were mechanically squeezed to release excess slurry and allowed to dry at room temperature. The process was repeated as necessary to generate enough scaffolds for testing.

3. Heat Treatment Profile

The coated foam templates were heat treated in a Thermo Scientific Lindberg Blue M furnace from room temperature to 400°C at 1°C/min and held for 1 hour to burn out the foam. The temperature was then increased to 650°C at 2°/min and held for 5 hours before cooling to room temperature at 5°C/min.

B.Scaffold Characterization

1. X-ray Diffraction (XRD)

Following heat treatment, scaffolds were crushed into a powder, mixed with isopropanol, and dispersed onto the surface of a sample holder. Diffraction patterns were generated using a Bruker D2 Phaser with Cu radiation, a voltage of 30 kV, and a 10 mA current. Diffractograms were collected on the range $10° < 2\theta < 80°$, with a step size of 0.03°, and a step time of 1 s. Crystalline phases were identified using Joint Committee for Powder Diffraction Studies (JCPDS) standard patterns.

2. Scanning Electron Microscopy/Energy Dispersive X-ray Spectroscopy (SEM/EDX)

Scaffolds were coated with gold palladium using a Cressington Sputter Coater 108. A Quanta 200F Environmental Scanning Electron Microscope was used to image the scaffolds under a vacuum at a pressure of 0.90 torr. An FEI EDAX system equipped with a silicon-drift detector was used to perform energy dispersive x-ray spectroscopy. The voltage ranged between 8.0 and 15.0 kV and the spot size was from 3.0 to 5.0. Images were taken both before and after SBF incubation.

3. Pore Diameter Measurements

An Olympus IX20-UCB Optical Fluorescent Microscope was used to estimate the pore diameter of the scaffolds at 4x magnification. Measurements were made using Image-Pro AMS 5.1 software with a 500 μm calibration standard. A total of 90 different measurements were made for each glass composition and the average and standard deviation were calculated.

4. Fluorescent Stereo Microscopy

A Leica M165 FC Fluorescent Stereo Microscope was used to take images of the scaffolds at 2x, 4x, and 8x magnification. Images were analyzed using LAS V4.8 software.

C. Simulated Body Fluid (SBF) testing

1. SBF Preparation

Simulated body fluid (SBF) was prepared in accordance with the procedure outlined by Kokubo et al[15].The reagents used to make SBF are outlined in Table 1. Reagents 1 to 8 were dissolved in order in 700 mL deionized water while stirring and heating at 36.5°C. Deionized water was added up to a total solution volume of 900 mL. Tris and 1M HCl were added in an alternating fashion to adjust the pH to 7.40. The solution was allowed to cool to room temperature before adding deionized water up to a total volume of 1000 mL. The prepared SBF was stored in plastic bottles in a 5°C refrigerator.

Table I: Amount and order of reagents used in SBF preparation

Order	Reagent	Amount
1	NaCl	8.035 g
2	$NaHCO_3$	0.355 g
3	KCl	0.225 g
4	$K_2HPO_4 \bullet 3H_2O$	0.231 g
5	$MgCl_2 \bullet 6H_2O$	0.311 g
6	1.0M-HCl	39 mL
7	$CaCl_2$	0.292 g
8	Na_2SO_4	0.072 g
9	Tris	6.118 g
10	1.0M-HCl	0-5 mL

2. Scaffold Incubation and Fluid Exchange

Scaffolds were sterilized by autoclaving at 121°C for 45 minutes steam time with 15 minutes dry time. Two scaffolds per composition (*n=2*) were placed in 12 well plates with 4 mL of SBF and placed in an incubator at 37°C for four time periods (*15, 30, 45, and 60 days*). Every 5 days, 2 mL of SBF was removed and exchanged for fresh SBF. The removed SBF was filtered and saved for later analysis. The pH of each solution was measured before SBF exchange usingan Acumen Excel XL15 pH meter.

3. Inductively Coupled Plasma – Optical Emission Spectroscopy (ICP-OES)

The filtered SBF from scaffold incubation was prepared in a 1:10 dilution with deionized water and the ion release profiles were analyzed using a Perkin Elmer Optima 8000 with an auto sampler. Ca, P, and Si were analyzed using calibration standards for 1, 10, and 100 ppm and the standards for Ti were 0.1, 1, and 10 ppm.

III. RESULTS

A. Characterization

The results for XRD analysis of the three compositions of bioactive glass scaffolds shown in Figure 3 indicate that *BG-4* had the most amorphous phase conserved post-sintering. The crystalline phases present in *Con* were $Na_2Ca_2(SiO_3)_3$ and $NaCaPO_4$ (sodium calcium phosphate). *BG-2* also had $Na_2Ca_2(SiO_3)_3$ present, but the second phase was a sodium calcium phosphate silicate compound ($Na_2Ca_4(PO_4)_2SiO_4$) while *BG-4* only showed evidence of the $Na_2Ca_4(PO_4)_2SiO_4$ crystalline phase. Stereo microscope images in Figure 3 support this data with a glassy appearance in *BG-4* not visible in *Con* or*BG-2*. Figure 4 shows closer images of BG-4 scaffolds, highlighting their glassy characteristic.

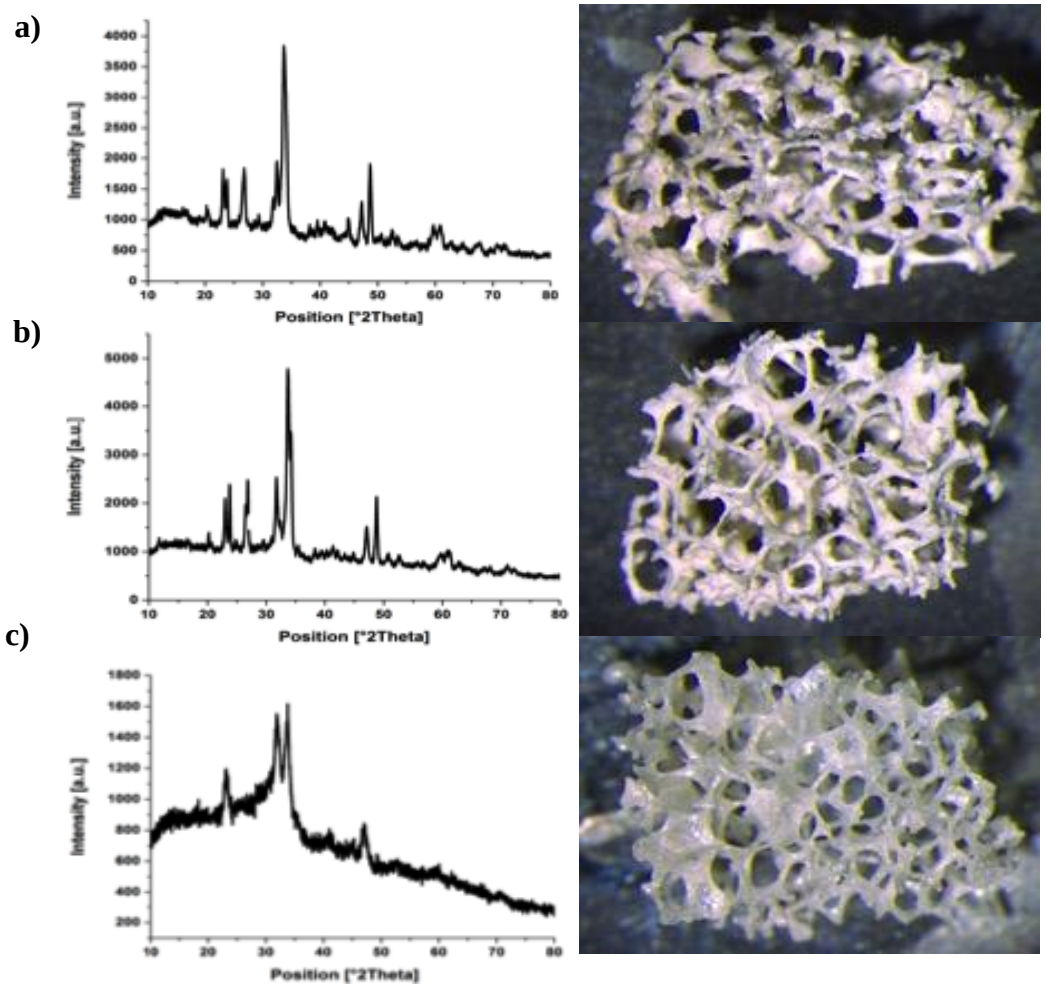

Figure 3: XRD patterns and stereo images of a) *Con*, b) *BG-2*, and c) *BG-4*

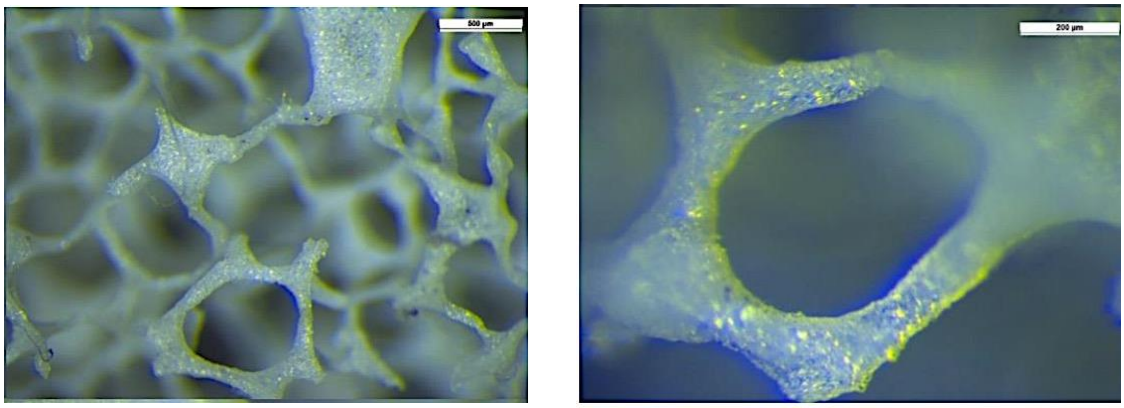

Figure 4: Stereo microscope images of *BG-4* showing its glassy nature

Optical microscopy images (Figure 5) further confirm the retained amorphous character in *BG-4* scaffolds through the transparency of the struts. These images also display the interconnected network of open pores with average diameters of 516 µm (±149), 524 µm (±143), and 533 µm (±125), respectively.

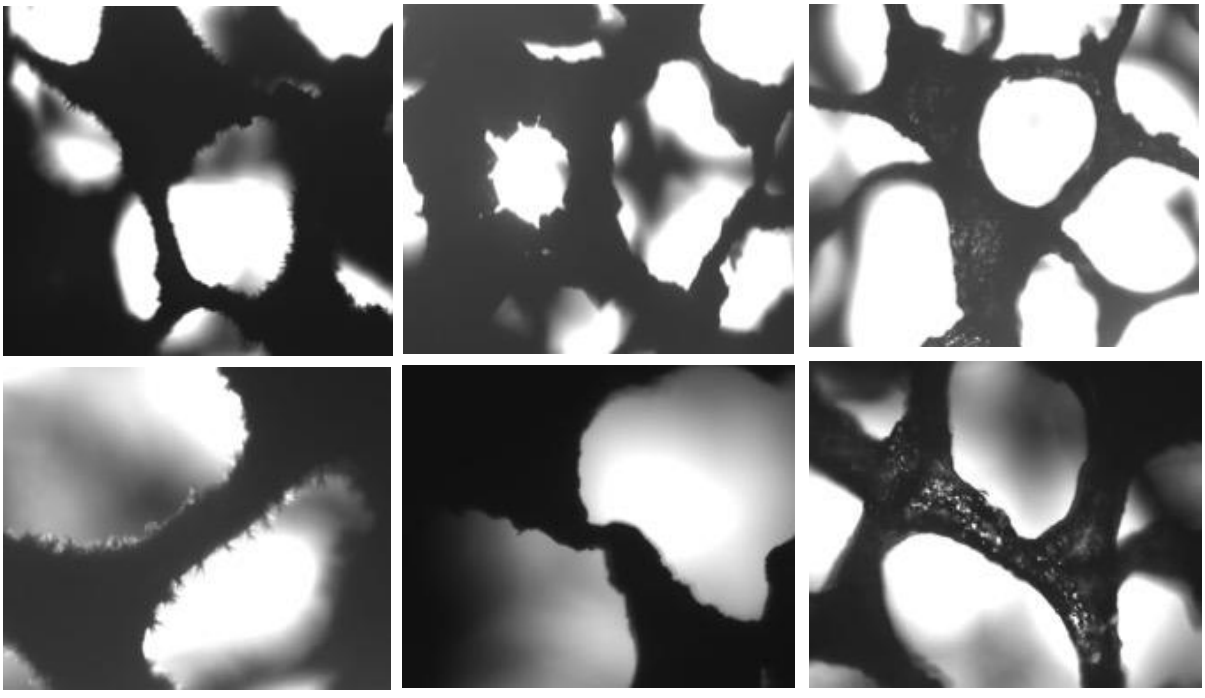

a) **b)** **c)**

Figure 5: Optical images of a) *Con*, b) *BG-2*, and c) *BG-4*

Initial SEM imaging of surface topography revealed needle-like projections on the surface of *Con* (Figure 6a) scaffolds, while *BG-2* (Figure 6b) had small rounded outgrowths and *BG-4* (Figure 6c) had similar rounded features but was smoother. SEM images confirmed the open pore network visualized in optical microscopy. EDX was used to analyze the chemical composition, with the presence of Si, Ca, Na, and P in all three scaffolds and the addition of Ti in *BG-2* and *BG-4*.

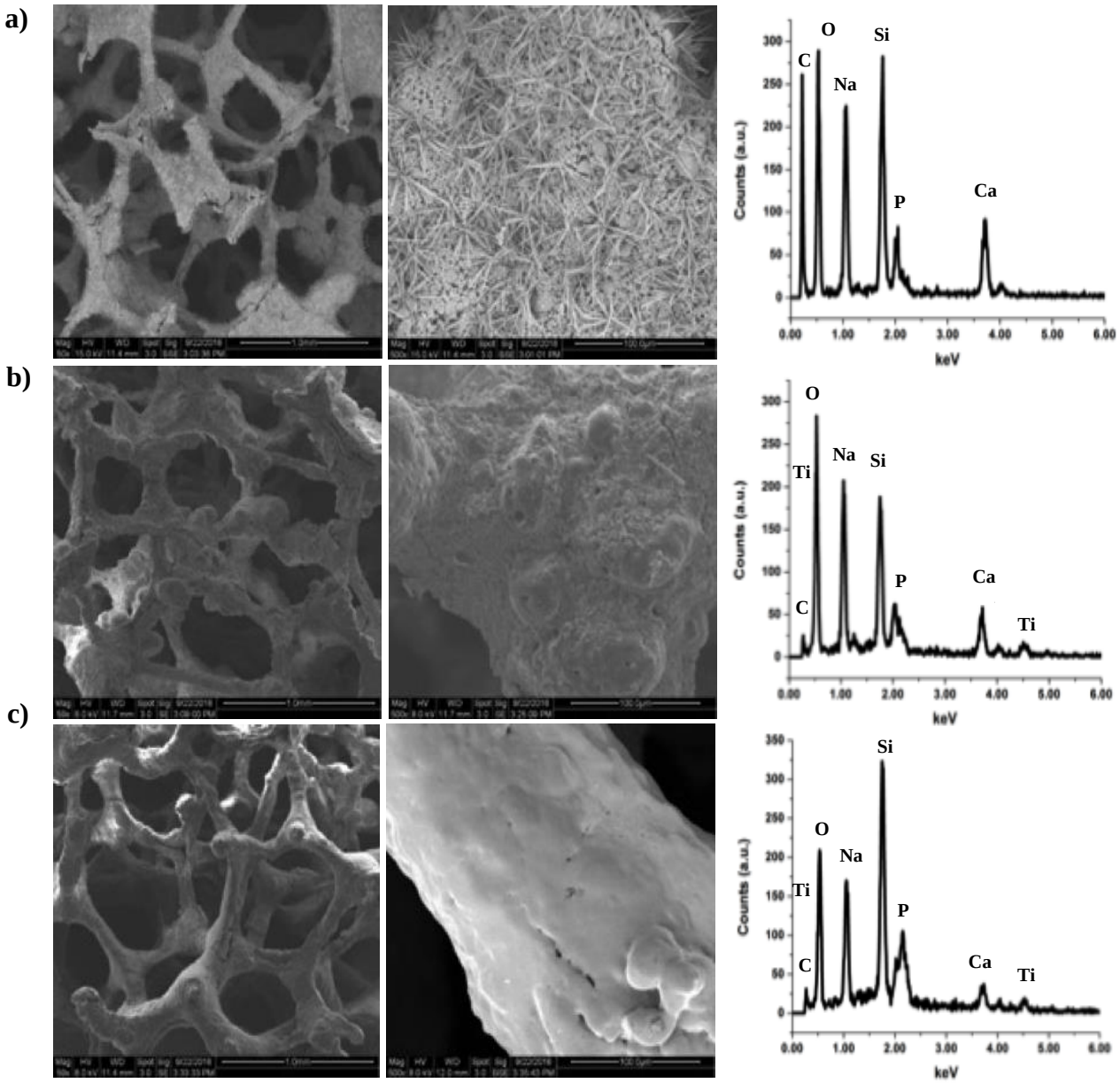

Figure 6: SEM images and corresponding EDX plots for a) *Con*, b) *BG-2*, and c) *BG-4*

B. Bioactivity

Bioactivity was assessed through scaffold incubation in SBF with pH measurements followed by SEM/EDX and ICP analysis. The pH was initially around 8.6 for *Con* and dropped to ~7.3 after 30 days, fluctuating around this value for the remainder of the 60 day time period. *BG-2* and *BG-4* followed similar patterns, but were initially close to 8.0 and 7.7, respectively, and oscillated around 7.4 from 30-60 days. Figure 7 shows the pattern of pH decrease over the 60 day time period.

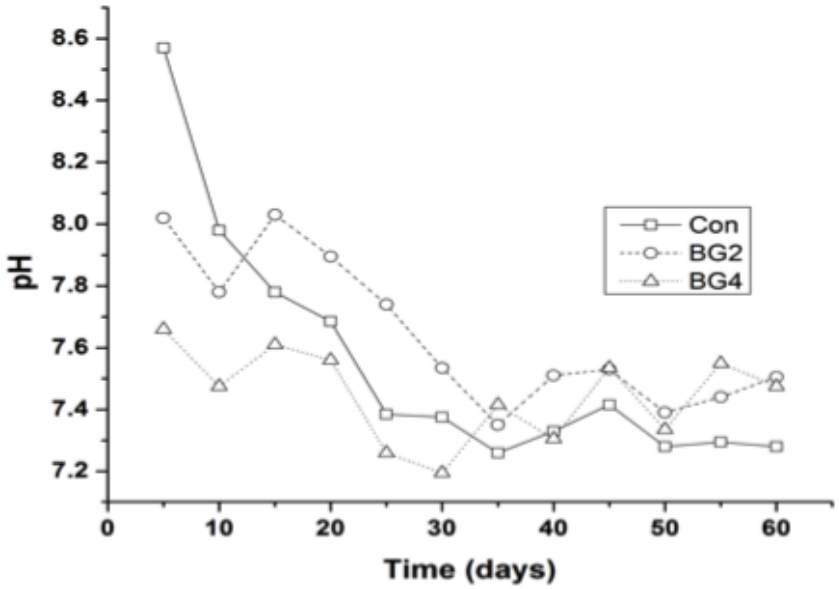

Figure 7: pH of SBF after scaffold incubation for 5-60 days

SEM/EDX revealed the presence of CaP crystals on *Con* scaffolds after 15 days with increasing surface coverage corresponding to increased SBF incubation time, while *BG-2* and *BG-4* did not show visible precipitation after 60 days. Figure 8 shows the post-incubation SEM images for 30 and 60 days with EDX analysis for 60 days.

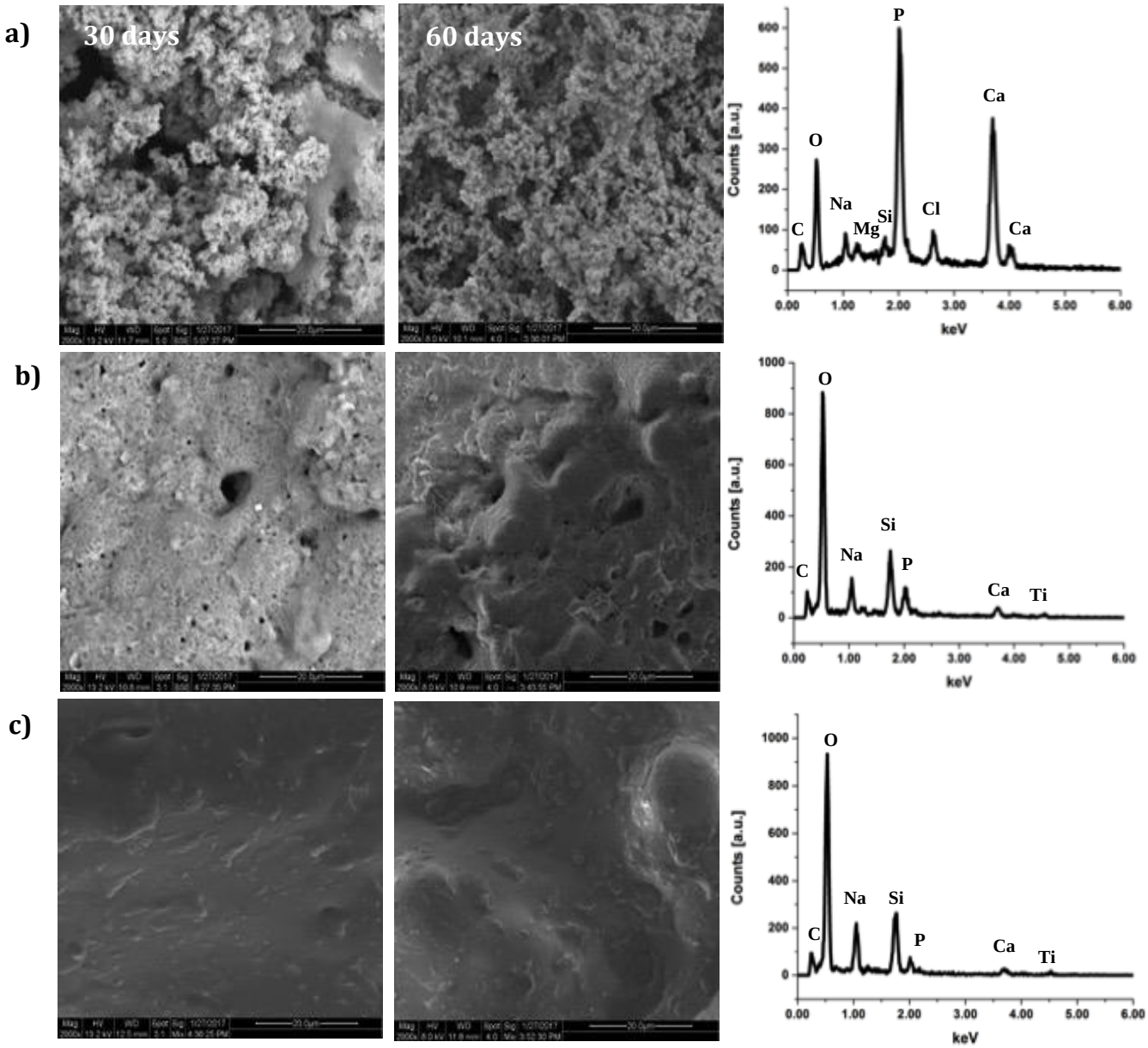

Figure 8: SEM images and EDX plots after SBF incubation for 30 and 60 days for a) *Con*, b) *BG-2*, and c) *BG-4*

Quantitative EDX values presented in Table II verified this result, as *Con* showed an increase from 16 wt% Ca and 9 wt% P prior to SBF incubation (0 days) up to 65 wt% Ca and 31 wt% P after 60 days. *BG-2* also showed an increase, although it was smaller in magnitude from 9 wt% to 22 wt% Ca and 8 wt% to 20 wt% P over the 60 day time period. With regards to *BG-4*, Ca increased from 6 wt% to 26 wt% Ca after 30 days, but

declined to 17 wt% after 60 days while P concentration followed an increasing trend from 7 wt% to 10 wt% to 11 wt% for 0, 30, and 60 day measurements.

Changes were also observed in the surface composition with respect to Na and Si concentrations for all three glasses. For *Con*, a decrease in both Na (29 wt% to 2 wt%) and Si (34 wt% to 2 wt%) was observed. *BG-2* also showed a decline in Na (32 wt% to 12 wt%), but an increase in Si content on the surface was detected (25 wt% to 32 wt%). The results for *BG-4* were different from both *Con* and *BG-2* in that the concentrations of Na and Si did not follow a steady up or down trend. Rather, there was an initial decrease accompanied by a corresponding increase up to just below the starting levels for the non-incubated scaffolds with Na (22 wt%, 13 wt%, 20 wt%) and Si (43 wt%, 29 wt%, 40 wt%) at 0, 30, and 60 days, respectively. Ti content of *BG-2* and *BG-4* was also noted with an overall increase during the trial.

Table II: Quantitative EDX results after 60 days SBF incubation

	Control			**BG2**			**BG4**		
Element (wt%)	***0 days***	***30 days***	***60 days***	***0 days***	***30 days***	***60 days***	***0 days***	***30 days***	***60 days***
Na	28.51	2.09	1.79	31.51	16.56	11.82	21.70	13.47	19.90
Si	34.34	9.92	1.94	24.56	26.87	31.84	43.04	29.24	39.75
Ca	15.82	60.46	65.20	8.54	10.14	22.00	5.74	25.73	17.35
P	8.74	27.53	31.07	7.92	14.46	20.49	7.06	9.68	11.29
Ti	-	-	-	2.86	4.38	13.86	2.56	21.88	11.71

In relation to the EDX results, ion release data shown in Figure 9 was collected to determine Si, Ca, P, and Ti precipitation in SBF through analysis with ICP-OES. *Con* (Figure 9a) had an initial Si release of 52 mg/L after 5 days that decreased to 4 mg/L after 15 days and then fluctuated around 30-40 mg/L for the remainder of the 60 days. Ca showed a similar pattern starting with a release of 242 mg/L at 5 days with a marked decrease by 10 days followed by stabilization in a range of approximately 30-50 mg/L for 20-60 days. P and Ti release were negligible for *Con*.

BG-2 (Figure 9b) displayed a comparable trend to *Con* with high ion release of Si and Ca after 5 days at 73 mg/L and 205 mg/L with a decrease to 10-46 mg/L and 60-85

mg/L respectively for the remainder of the 60 days. While *BG-2* had a higher initial release of Si than *Con*, it decreased to approximately the same level in both glasses while less Ca was released in *BG-2* to start with, but maintained a higher release range for the rest of the cycle. Ti release was also negligible in *BG-2*, while P was detected at levels <16 mg/L.

BG-4 (Figure 9c) displayed a distinct ion release profile when compared to *Con* and *BG-2*. There was an initial Si release of 9 mg/L after 5 days that decreased to 0 mg/L for the remainder of the trial. Ca release was significantly lower than in *Con* or *BG-2* at 134 mg/L initially, but hit a minimum at 58 mg/L after 20 days and climbed back up to around the starting release level, ending at 91 mg/L. P showed much greater release starting at 43 mg/L, as compared to an absence of P release in *Con* and <16 mg/L in *BG-2* with a peak at 45 mg/L after 55 days before falling to a final concentration of 25 mg/L. Ti release was again found to be nearly undetectable.

a)

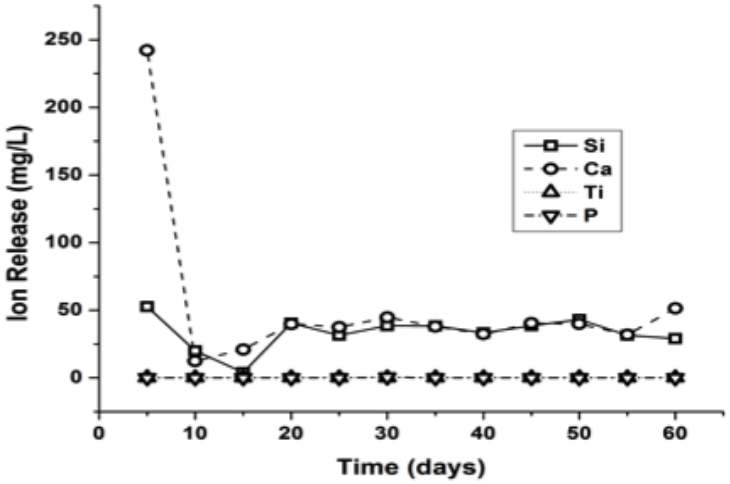

b)

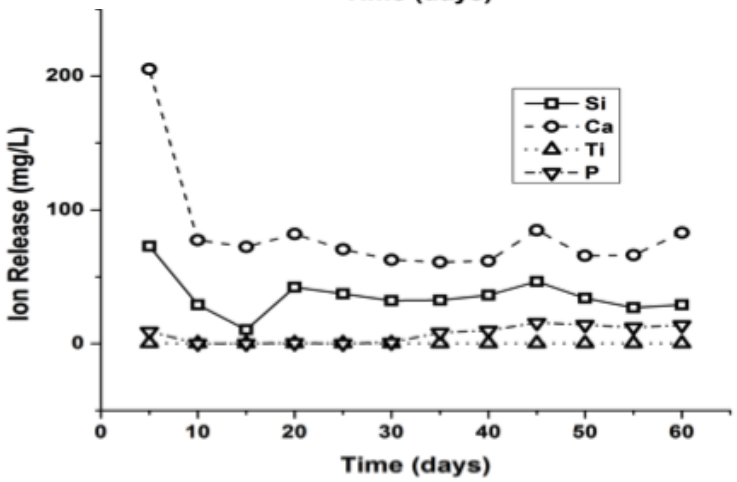

c)

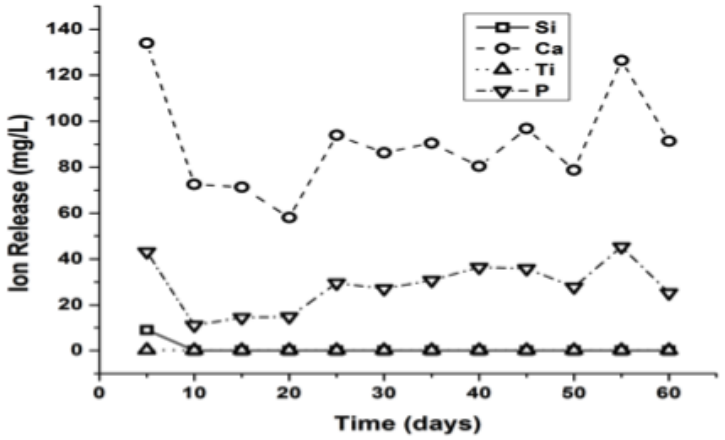

Figure 9: Ion release of Si, Ca, Ti, and P after 60 days for a) *Con*, b) *BG-2*, and c) *BG-4*

IV. DISCUSSION

A. Characterization

Results from XRD analysis showed the presence of a sodium calcium silicate phase in both *Con* and *BG-2*. Previous studies have shown that sodium calcium silicate formation in bioactive glass is a typical aspect of the sintering process and does not inhibit the bioactivity or bone-bonding properties[16-17]. Other studies have indicated that composites of Bioglass® ($45SiO_2$-$24.5Na_2O$-$24.5CaO$-$6P_2O_5$) with other materials can produce a sodium calcium phosphate phase similar to the second crystalline phase observed in *Con*[18]. While mechanical properties of the scaffolds were not tested, an increase in strength was perceived with increasing amounts of Ti in the glass composition; *BG-4* had the highest resistance to pressure exerted on it during handling. The sodium calcium phosphate silicate in *BG-2* and *BG-4* may account for this increased resistance, as calcium silicate-sodium phosphate salts used in orthodontic brackets were found to have a shear bond strength comparable to that of tooth enamel[19].

Fewer crystalline peaks in the diffractogram for *BG-4* as compared to *Con* and *BG-2* XRD patterns, along with the glassy appearance in the *BG-4* stereo image (Figures 3 and 4) and the transparent appearance of the *BG-4* struts with optical microscopy (Figure 5) indicates the retained amorphous character is the highest in *BG-4* scaffolds. This evidence suggests that while all three compositions were heated about their glass transition temperatures (T_g) to condense into the porous structure, less of the crystallization process had been completed for *BG-4* scaffolds at the sintering temperature used in this study (650°C). While completely crystallized glass ceramics have been studied extensively due to their improved mechanical properties through powder compaction above the crystallization temperature, fewer solubility and protein adsorption effects have been reported[5-7,20]. This result leads to the need for longer incubation periods in body fluid to induce hydroxyapatite formation and thus promote bone-bonding ability[20]. A delay in the integration of the crystalline material into the host tissue demonstrates the applicability of fabricating scaffolds with less crystallinity and highlights the potential viability of *BG-4* scaffolds for protein and cell adhesion studies.

The confirmation of interconnected open pore networks with optical (Figure 5) and SEM (Figure 6) images shows that the scaffolds have a structural arrangement compatible for cell growth[12]. The pore diameters of 516 µm (*Con*), 524 µm (*BG-2*), and 533 µm (*BG-4*) show that while there is a minor enlargement of pore size with increasing Ti content, they are still within a 20 µm range. Additionally, the pore diameters are slightly larger than the maximum size (500 µm) for optimal cell seeding and nutrient exchange in bone tissue engineering[12]. However, large standard deviations (>100 µm) in the measurements for the scaffolds in this study indicate that there is a wide variation of pore sizes, suggesting that at least some of the pores will be viable for supporting tissue development.

SEM images prior to SBF incubation (Figure 6) show the unmodified surface morphology of the post-sintered glasses. The needle-like projections on *Con* could be the result of the interactions between constituent elements during the heating process. The progressive smoothness on *BG-2* and *BG-4* glasses could arise from the flow-like state of glasses observed when held near their glass transition temperatures for long periods of time.This viscoelasticity improves bonding ability between glass particles to form a cohesive structure. EDX verified the presence of Si, Na, Ca, and P in all three glasses and Ti in *BG-2* and *BG-4*.

B. Bioactivity

Scaffolds post-incubation in SBF were analyzed with SEM/EDX (Figure 8) to reveal CaP deposition on *Con* surfaces by 15 days, with increasing amounts at longer time periods. This result was not unexpected, as the formation of a CaP coating on bioactive glass structures of a similar composition has been observed in the form of a hydroxyapatite layer since the first *in vitro* and *in vivo* trials with Bioglass®[7]. The lack of visible CaP deposition on *BG-2* and *BG-4* can be justified by evaluating the interface between Bioglass® particles and Ti-based implants. A strong interaction between Bioglass® coatings on Ti alloys made of Ti6Al4V has been reported[21]. This information suggests that the incorporation of Ti into the glass structure could enhance the efficacy of bond strengths within the glass, thus lowering the probability of CaP dissolution from the

glass network to form a surface layer. However, quantitative EDX data shows some increase in the amount of Ca and P for *BG-2* and *BG-4*, indicating that there may be a thin film of CaP on the surface.

SBF testing was performed to evaluate the surface reactivity of the scaffolds in an environment created to resemble the conditions within the body. Previous research reports the formation of CaP crystals on Ti-containing bioactive glasses; however, Ti was present in lower concentrations (<4 wt%) as compared to 12 wt% and 24 wt% used in *BG-2* and *BG-4* and SBF testing was done in static conditions[22]. In this study, half of the fluid used to immerse the scaffolds was exchanged every 5 days to mimic the dynamic flow of material throughout the circulatory system. An implanted biomaterial would be subject to the constant movement of ions and other dissolved substances into and out of the region, thus validating the use of this method. De Aza et al. reported the use of a dynamic flow technique for SBF incubation of a tricalcium phosphate (TCP)[23]. They concluded that while HA deposition was present in the static study and not in the dynamic testing, the dynamic study was a better representation of *in vivo* conditions[23]. These results indicate that the absence of CaP deposition on Ti-containing scaffolds is a likely representation of the potential outcome of clinical trials and suggests modification of the glass composition to promote CaP formation. It is plausible that the use of a dynamic flow study also had an influence on the results for pH (Figure 7), as the initial pH decreased gradually until it stabilized within a small range around ~7.4 for each glass.

The initially high Si and Ca release from *Con* (52 mg/L, 242 mg/L) and *BG-2* (73 mg/L, 205 mg/L) indicates the relative weakness of the glass network in these structures, as they rapidly liberate ions when immersed in fluid before leveling off (Figure 9). The low Si release and initially low Ca release in *BG-4* showed that it had a stronger structure taking more time for dissolution of Ca, as indicated by the increasing Ca release near the end of the 60 day time period. This trend, along with the similar increasing release of P at this point in the time trial, suggests that a longer incubation period may lead to CaP deposition. The stronger network could be attributed to the formation of P-O-Ti and/or

Si-O-Ti bonds within the glass that have been observed at high Ti concentrations where it may act as a network former[24].

V. CONCLUSIONS

The objectives of this study were to characterize scaffolds fabricated from a series of $42SiO_2$-$24Na_2O$-$21CaO$-$14P_2O_5$ wt% glass compositions with incremental substitutions of TiO_2 for SiO_2 and evaluate the biocompatibility of the structures. XRD indicated more crystallinity in glasses with low or no TiO_2, while scaffolds with a high concentration of TiO_2 were partially amorphous. Microscopic methods revealed a structural network of interconnected open pores with pore diameters slightly greater than 500 μm. Incubation in SBF showed the presence of a CaP layer on scaffolds without Ti, while no deposition was visible on Ti-containing scaffolds. Ion release data showed high initial output of Si and Ca from *Con* and *BG-2* scaffolds that rapidly tapered off. Reduced ion release from *BG-4* scaffolds indicated stronger bonds between Ti and other elements in the glass composition.

VI. SUGGESTIONS FOR FUTURE WORK

Future work could focus on the mechanical properties of the scaffolds, including hardness and compression testing. Optimizing these qualities can be accomplished by matching the strength of the scaffold to its specific application. Cytocompatibility determination will also be an important direction for future study to further evaluate the biocompatibility of the scaffolds and establish their potential for attracting cells to regenerate damaged tissue. Additionally, adjusting the level of Ti or increasing SBF incubation periods to induce the formation of a hydroxyapatite layer on the surface may be beneficial for bone-bonding ability.

VII. LITERATURE REFERENCES

1. D. F. Williams, "On the nature of biomaterials," *Biomaterials,* **30**, 5897-5909 (2009).

2. "Boom time for biomaterials," *Nat. Mater.*, **8** (2009).

3. B. D. Ratner, A. S. Hoffman, F. J. Schoen, and J. E. Lemons, *Biomaterials Science – an Introduction to Materials in Medicine*; pp. 37-105. Academic Press, San Diego, CA, 1996.

4. J. D. Enderle, S. M. Blanchard, and J. D. Bronzino, *Introduction to Biomedical Engineering*; p. 263. Elsevier Academic Press, Burlington, MA, 2005.

5.M. N. Rahaman, D. E. Day, B. S. Bal, Q. Fu, S. B. Jung, L. F. Bonewald, and A. P. Tomsia, **"**Bioactive glass in tissue engineering," *Acta Biomater*., **7**[6], 2355-73 (2011).

6.J. R. Jones,"Review of bioactive glass: From Hench to hybrids," *Acta Biomater*., **9**, 4457-86 (2013).

7. L. L. Hench, "The story of Bioglass®," *J. Mater. Sci: Mater. Med.,* **17**, 967-78 (2006).

8. A. Hoppe, N. S Güldal, and A. R. Boccaccini,"A review of the biological response to ionic dissolution products from bioactive glasses and glass-ceramics," *Biomaterials*, **32**, 2757-74 (2011).

9. S. K. Nandi, A. Mahato, B. Kundu, and P. Mukherjee, *Doped bioactive glassmaterials in bone regeneration, Advanced Techniques in Bone Regeneration*, Ch. 13. InTech, 2016.

10.A. W. Wren, A. Coughlan, K. E. Smale, S. T. Misture, B. P. Mahon, O. M. Clarkin, and M. R. Towler, "Fabrication of $CaO–NaO–SiO_2/TiO_2$ scaffolds for surgical applications," *J. Mater. Sci:Mater. Med.,* **23**, 2881-91 (2012).

11.L. L. Hench, "Chronology of bioactive glass development and clinical applications," *New J. Glass Ceram.*,**3**, 67-73 (2013).

12. L. Gerhardt and A. R. Boccaccini. "Bioactive glass and glass-ceramic scaffolds for bone tissue engineering," *Materials.* ,**3**, 3867-910 (2010).

13.R. H. Carmona, "Bone Health and Osteoporosis: a Report of the Surgeon General," U.S. Department of Health and Human Services, WE-225-B71259, 436 pp. (2004).

14.M. M. Stevens,"Biomaterials for bone tissue engineering,"*Mater. Today*, **11** [5], 18-25 (2008).

15. T. Kokubo and H. Takadama, "How useful is SBF in predicting in vivo bone bioactivity?" *Biomaterials,* **27**, 2907-2915 (2006).

16. H. A. ElBatal, M. A. Azooz, E. M. A. Khalil, A. S. Monem, and Y. M. Hamdy, "Characterization of some bioglass-ceramics," *Mater. Chem. Phys.*, **80**, 599-609 (2003).

17. R. Xin, Q. Zhang, and J. Gao, "Identification of the wollastonite phase in sintered 45S5 bioglass and its effect on in vitro bioactivity," *J. Non-Cryst. Solids,* **356**, 1180-84 (2010).

18. H. Demirkiran, A. Mohandas, M. Dohi, A. Fuentes, K. Nguyen, and P. Aswath, "Bioactivity and mineralization of hydroxyapatite with bioglass as sintering aid and bioceramics with $Na_3Ca_6(PO_4)_5$ and $Ca_5(PO_4)_2SiO_4$ in a silicate matrix," *Mater. Sci. Eng. C*, **30**, 263-72 (2010).

19. A. Costenoble, E. Vennat, J.-P. Attal, and E. Dursun, "Bond strength and interfacial morphology of orthodontic brackets bonded to eroded enamel treated with calcium silicate–sodium phosphate salts or resin infiltration," *Angle Orthodontist,* **86** [6], 909-16 (2016).

20. M. S. Bahniuk, H. Pirayesh, H. D. Singh, J. A. Nychka, and L. D. Unsworth, "Bioactive Glass 45S5 Powders: Effect of Synthesis Route and Resultant Surface Chemistry and Crystallinity on Protein Adsorption from Human Plasma," *Biointerphases*, **7**, 41 (2012).

21. J. M. Gomez-Vega, E. Saiz, A. P. Tomsia, G. W. Marshall, and S. J. Marshall, "Bioactive glass coatings with hydroxyapatite and Bioglass particles on Ti-based implants. 1. Processing," *Biomaterials,* **21**, 105-111 (2000).

22. A. W. Wren, N. M. Cummins, F. R. Laffir, S. P. Hudson, and M.R. Towler, "The bioactivity and ion release of titanium-containing glass polyalkenoate cements for medical applications," *J. Mater. Sci: Mater. Med.*, **22**, 19-28 (2011).

23. A. H. De Aza, P. Velásquez, M. I. Alemany, P. Pena, and P. N. De Aza, "In Situ bone-like apatite formation from a bioeutectic ceramic in SBF dynamic flow," *J. Am. Ceram. Soc.*, **90** [4], 1200-1207 (2007).

24. F. Taloş, M. Senilă, T. Frentiu, and S. Simon, "Effect of titanium ions on the ion

release rate and uptake at the interface of silica based xerogels with simulated body fluid," *Corros. Sci.*, **72**, 41-46 (2013).